

Independent determination of symmetry and polarity in the *Drosophila* eye

(ommatidia/photoreceptor/mirror symmetry/equator)

KWANG-WOOK CHOI*, BRIAN MOZER†, AND SEYMOUR BENZER‡

Division of Biology, California Institute of Technology, Pasadena, CA 91125

Contributed by Seymour Benzer, February 16, 1996

ABSTRACT In each facet of the *Drosophila* compound eye, a cluster of photoreceptor cells assumes an asymmetric trapezoidal pattern. These clusters have opposite orientations above and below an equator, showing global dorsoventral mirror symmetry. However, in the mutant *spiny legs*, the polarization of each cluster appears to be random, so that no equator is evident. The apparent lack of an equator suggests that *spiny legs*⁺ may be involved in the establishment of global dorsoventral identity that might be essential for proper polarization of the photoreceptor clusters. Alternatively, a global dorsoventral pattern could be present, but *spiny legs*⁺ may be required for local polarization of individual clusters. Using an enhancer trap strain in which *white*⁺ gene expression is restricted to the dorsal field, we show that *white*⁺ expression in *spiny legs* correctly respects dorsoventral position even in facets with inappropriate polarizations; the dorsoventral boundary is indeed present, whereas the mechanism for polarization is perturbed. It is suggested that the boundary is established before the action of *spiny legs*⁺ by an independent mechanism.

Pattern formation in multicellular organisms involves precise processing of positional information and cell–cell interactions. The *Drosophila* compound eye has been a model for studying pattern formation because it consists of repetitive arrays of about 800 unit eyes (ommatidia) containing identical sets of photoreceptors and accessory cells. Each cluster of eight photoreceptors (R1–R8) is assembled in a trapezoidal pattern with characteristic anterior–posterior (A/P) and dorsoventral (D/V) planar polarity in the retinal epithelium. In the A/P axis, R1–R2–R3 cells are anterior to the R5–R6 cells. With respect to the D/V axis, R3–R4–R5 cells are polar (see Fig. 1).

Although each individual photoreceptor cluster is asymmetric, the eye as a whole displays a global mirror symmetry; the trapezoids in the dorsal half of the eye are mirror images to those in the ventral half, establishing global symmetry about the equatorial midline. This mirror symmetry develops during eye morphogenesis, as photoreceptor clusters rotate 90° in opposite directions above and below the equator (1, 2). Genes such as *nemo* and *roulette* are required for proper rotation of the photoreceptor clusters (3).

The retinal precursor cells in the dorsal and ventral fields do not arise from different cell lineages since mosaic clones can be generated that extend to the other side of the equator. Little is understood of how the global D/V fields are specified in the developing eye. Interestingly, *P-lacW* enhancer trap strains (4) have been isolated by us and others (5, 6) that express the *white*⁺ (*w*⁺) gene contained in the P-element strictly in the dorsal field of an eye. The dorsal specificity of *w*⁺ expression in such lines suggests that there are genetic mechanisms that specify either dorsal or ventral expression of genes. Because the eye displays dorsoventral distinctions at two levels, (i) the

polarity of an individual ommatidium and (ii) the global D/V mirror symmetry, the question is raised whether they are determined by independent mechanisms.

The *Drosophila* adult eye develops from the eye imaginal disc, which has a single layer of epithelium. The differentiation of retinal cells begins at the posterior margin of the disc and proceeds anteriorly. The formation of photoreceptor clusters and their subsequent rotation are initiated closely behind the morphogenetic furrow, an indentation of apical epithelium that marks the wave of differentiation in the eye. Progression of the furrow is regulated by a series of signaling events that require molecules encoded by *hedgehog* (*hh*), *decapentaplegic* (*dpp*), *patched* (*ptc*), and the gene encoding a major protein kinase A (*DCO*) (7–12). Ectopic expression of *hh* or clonal loss of *DCO* or *ptc* function results in the induction of ectopic furrows (11, 12) as well as ectopic equators (5). These studies suggest that the direction of furrow progression plays an important role in controlling both ommatidial polarity and equator. However, it is unclear whether ommatidial polarity and more global determinants are determined by the same mechanisms.

Morphogenetic processes involved in cuticular polarity formation have been studied using strains referred to as “polarity” mutants that have altered orientations of hairs and bristles (13). Interestingly, some polarity mutants, including *spiny legs* (*sple*) (14, 15), *dishvelled* (*dsh*) (16), and *frizzled* (*fz*) (17, 18), also show abnormal polarity of the photoreceptor clusters, providing some clues to study genetic mechanisms underlying the ommatidial polarity formation.

Among several polarity mutants, *sple* shows remarkably specific pattern defects: the majority of abnormal ommatidia in the *sple* eye are only dorsoventrally reversed and show complete 90° rotations, whereas *fz* shows a mixture of eye phenotypes such as D/V and A/P reversals and incomplete rotation (19). We have isolated a *P-lacW* enhancer trap strain in which *w*⁺ gene expression is restricted to the dorsal domain providing a useful D/V marker. We here address the relationship between the global mirror symmetry and the local ommatidial polarity, using the mutant *sple* and the *P-lacW* enhancer trap marker.

MATERIALS AND METHODS

Fly Stocks. *B1-12* was isolated from an enhancer trap screen (unpublished results) using the procedure described in Bier *et al.* (4). *B1-12* contains a single *P-lacW* insertion at the 69 D region of the third chromosome (data not shown). Homozygosity for *B1-12* causes lethality. Occasionally (less than 1%),

Abbreviations: A/P, anterior–posterior; D/V, dorsoventral.

*Present address: Department of Cell Biology, Baylor College of Medicine, Houston, TX 77030.

†Present address: Laboratory of Molecular Biology, National Institutes of Health, Bethesda, MD 20892.

‡To whom reprint requests should be addressed. e-mail: benzer@caltech.edu.

The publication costs of this article were defrayed in part by page charge payment. This article must therefore be hereby marked “advertisement” in accordance with 18 U.S.C. §1734 solely to indicate this fact.

homozygous escapers were found that show the same dorsal pattern of eye pigmentation as the heterozygotes. The *sple*¹ allele was provided by the Indiana stock center. *sple* flies were crossed to *yw*; *B1-12/TM3 Sb* to generate *yw*; *sple*; *B1-12/TM3Sb* flies. All markers and balancers are described in Lindsley and Zimm (20).

Histology and Immunohistochemistry. For light microscopic analysis, adult fly heads were fixed [1% glutaraldehyde/1% paraformaldehyde in 100 mM phosphate-buffered saline (PBS), pH 7.5], embedded in EMbed-812 (EM Sciences, Fort Washington, PA). The eyes were serially sectioned at 1 μ m. For immunohistochemistry, third instar eye discs were fixed in periodate-lysine-paraformaldehyde fixative (21) and stained with a 1:50 dilution of an anti-Bar antibody (S12) (22) as described (23). Secondary antibody was a 1:50 dilution of horseradish peroxidase-conjugated anti-rabbit IgG. After rinsing in PBS, they were stained with diaminobenzidine (0.5 mg/ml) containing 0.04% NiCl.

RESULTS

Dorsoventral Reversals in *spiny legs*. Local polarity reversals in *sple* mutants were demonstrated (15) by an optical neutralization technique (24). For better resolution of the photoreceptor clusters, we examined tangential sections of *sple* eyes, confirming that many photoreceptor clusters showed local reversals of D/V polarity. Occasional A/P reversals also occurred, but at a much lower frequency (Fig. 1; Table 1). Remarkably, no abnormality was apparent in the number of photoreceptor cells per ommatidium or in the regular, hexagonal ommatidial array. As can be seen in Fig. 1, the polarities were close to random in both the upper and lower halves of the eye; an equator axis for D/V mirror symmetry could not be drawn. The frequency of polarity reversals was estimated at 45% of 531 ommatidia scored in eyes of three different individuals. A/P reversals occurred at a rate of only 1%. Since *sple*¹ is a genetically null allele (13), the observed phenotype is likely due to complete loss of *sple* function. D/V reversals in *sple*¹ were also found by Zheng *et al.* (19). However, they were able to detect the equator as if their strain is phenotypically weaker than ours. One plausible explanation is that their *sple*¹ stock might have modifier(s) resulting in incomplete penetrance.

At first glance, *sple* eyes appear to have domains of ommatidia with the same orientation (Fig. 2A and B), which would suggest a degree of cooperative determination of polarity. We tested this by using a coin toss to assign heads or tails to each facet array. This yielded very similar pseudo-domains (Fig. 2C). Therefore, the polarity in each *sple* facet would appear to be independent of its neighbors. This is consistent with autonomous nature of *sple* function in the mosaic clones (19).

Ommatidial Polarity Is Independent of Global D/V Pattern. A marker for D/V distinction in the eye was provided by a *P-lacW* strain we isolated, *B1-12*, in which the *w*⁺ gene of the P-element is expressed only in the dorsal domain. Eye color is mainly due to pigment granules in the secondary pigment cells that surround the photoreceptor clusters. Normally, the *w*⁺ gene is expressed autonomously in the entire eye. However, in the *B1-12* strain, *w*⁺ expression is specifically abolished in the ventral domain (Fig. 3); within the dorsal field, *w*⁺ expression is slightly stronger in the anterior. The *w*⁺ expression of the small pigment granules within the photoreceptor cells is also restricted to the dorsal region (Fig. 3E).

At the equator, a line of pigment cells is shared by the dorsal and ventral fields. We examined (in the absence of the *sple* mutation) whether the pigment expression boundary in *B1-12* coincided precisely with the equator. While the coincidence was close, there were some departures. In all 10 eyes examined, ommatidia in the first row dorsal to the equator (as defined by the mirror symmetry of photoreceptor cluster polarity) often showed no detectable *w*⁺ expression or did so only in a subset

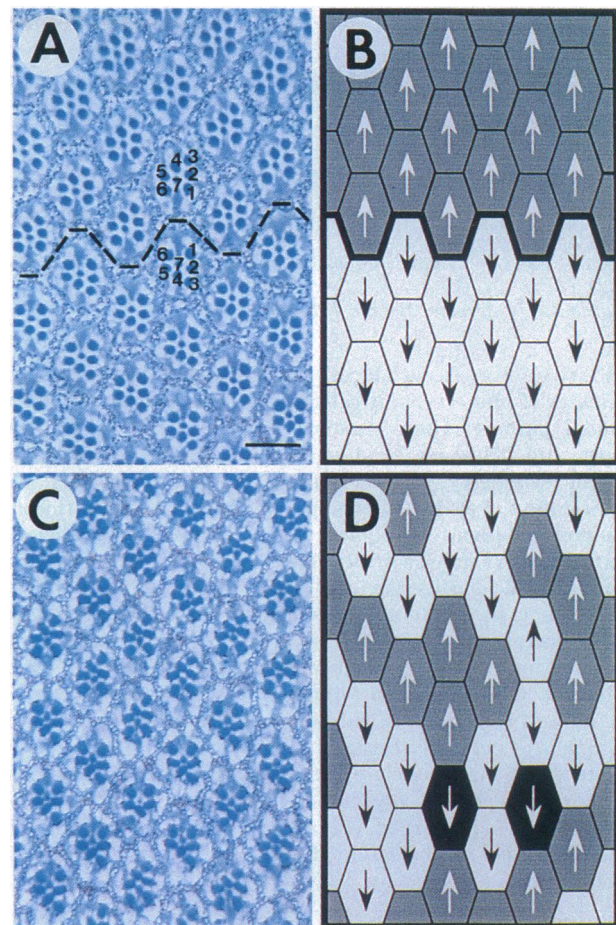


FIG. 1. Patterns of photoreceptor clusters in wild-type and *sple* mutant eyes. Adult eyes were embedded in EMbed resin, serially sectioned at 1 μ m, and stained with toluidine blue. (A) Photoreceptor cluster in the wild-type eye, showing the trapezoidal arrangement in each facet of the rhabdomeres of photoreceptors R1–R7 (R8, located underneath R7, does not appear at this plane of section). Photoreceptor clusters are surrounded by a hexagonal lattice of pigment cells. Note that R1, R2, and R3 are on the long, vertical anterior face of each trapezoid; R5 and R6 are on the short, vertical posterior. The horizontal dotted line represents the equator of mirror symmetry. The R7 rhabdomere projects into the middle of a cluster, between R1 and R6. (B) Using the projection of R7 as a convenient marker for orientation of each photoreceptor cluster, ommatidia with dorsal or ventral orientation are indicated in grey or white, respectively. (C) In the eye of a *sple* mutant, the hexagonal array of ommatidia, the number of cells per cluster, and their trapezoidal pattern are normal. However, many clusters show reversed polarity. (D) Schematic representation of C. No equator of symmetry is evident. Almost all reversals are dorsoventral, but rare A/P reversals also occur (solid areas). The anterior is to the right. (Bar = 10 μ m.)

of the pigment cells (Fig. 3). In some cases, the *w*[−] area extended as high as three rows above the equator. This suggests that, in *B1-12*, *w*⁺ expression may be specifically inhibited in the ventral eye field, the inhibition being mediated by a diffusible factor that can act at a distance up to three ommatidial rows. Nevertheless, *w*⁺ expression in this strain provides an approximate marker for an equator independently of the mirror symmetry of photoreceptor cluster polarity.

This enabled us to address the question whether D/V identity indicated by *w*⁺ expression and photoreceptor cluster polarity respond to the same cues. If so, when *sple* and *B1-12* are combined, polarity and *w*⁺ expression should be reversed together, i.e., ommatidia in the dorsal eye that have ventral polarity should be *white* and vice versa.

Table 1. Frequencies of polarity reversals in *sple* eyes

	Dorsal domain			Ventral domain		
	Normal	D/V switch	A/P switch	Normal	D/V switch	A/P switch
Eye 1	75	63	2	32	30	0
Eye 2	25	23	1	46	48	1
Eye 3	43	34	3	62	43	0
Total	143 (53%)	120 (45%)	6 (2%)	140 (54%)	121 (46%)	1 (0.4%)

sple flies were crossed to *yw; B1-12/TM3 Sb* to generate *yw; sple; B1-12/TM3 Sb*. Three eyes, each from a different fly, were sectioned and scored for D/V or A/P reversals. Dorsal and ventral domains were defined by the *w⁺/w⁻* pigmentation boundary. Note, in wild-type eyes, both D/V and A/P polarity reversals are very rare; among 523 ommatidia scored from three eyes, each from a different fly, there were three D/V reversals (0.6%) and no A/P reversals.

The result was that the pattern of photoreceptor geometry in the *B1-12* strain containing the *sple* mutation (*sple; B1-12/TM3 Sb*) was identical to that of *sple*, i.e., essentially random dorsal and ventral polarities. Similarly, the *sple* mutation did not change the dorsal specific *w⁺* expression (Fig. 4), showing that a global dorsoventral signal is clearly intact in the *sple* eye. Thus, *sple⁺* function is not involved in establishing the distinction between dorsal and ventral eye field. It is suggested that D/V identity is established early and *sple⁺* acts later to regulate polarization of photoreceptor clusters.

D/V Reversals in Developing *sple* Retina. The formation of polarity in photoreceptor clusters can be observed early in the eye imaginal disc of the third instar larva. To observe this in the *sple* mutant, we used the anti-BarH1 antibody S12, which recognizes BarH1 and BarH2 homeobox-containing proteins in the nuclei of photoreceptor cells R1 and R6 (22). In wild-type discs, the photoreceptor clusters showed, with only a few exceptions, two stained cells at the typical positions of R1 and R6 (Fig. 5A). Eye morphogenesis is initiated at the posterior end of the disc and proceeds to the anterior, with cells R1 and R6 joining the cluster after the preclusters containing R2, R3, R4, R5, and R8 have been formed (25). Therefore, anti-BarH1 staining begins several columns posterior to the furrow, and R1 and R6 serve as markers for the orientation of the cluster. In *sple* eye discs, as in wild-type discs, the antibody showed two cells per ommatidium, but the positions of R1 and R6 in many clusters were perpendicular to their normal positions (Fig. 5B). These would appear to be early forms of the ommatidia destined to show D/V reversals of rhabdomere pattern in the adult mutant eye.

Events that could lead to the anomalies in the *sple* eye disc are shown in Fig. 5C. Consider the possibility that, in *sple*, the fate of each photoreceptor cell is correctly specified, but the

cluster rotates in a random direction rather than adhering to the normal counterclockwise turn in the upper half of the eye and clockwise below (Fig. 5Cii). That cannot explain the *sple* phenotype because, if a cluster rotates in a reversed direction, the trapezoidal assembly of photoreceptors will become reversed not only dorsoventrally, but also anteroposteriorly. However, this is not the case in *sple* eyes, which show massive D/V pattern reversals, whereas A/P reversals are rare (Table 1).

An alternative possibility that may be more plausible is that in *sple* the photoreceptor clusters rotate normally in the upper and lower halves, but the fates of dorsal and ventral cells within a cluster are interchanged (Fig. 5Ciii). In normal development, the photoreceptor clusters initially are horizontally symmetrical; R1, R2, and R3 are dorsal and R4, R5, and R6 are ventral. The trapezoidal asymmetry develops at a later stage, after a 90° rotation (26), with R1, R2, and R3 becoming anterior and R4, R5, and R6 becoming posterior. An interchange of fate between R1, R2, and R3 with their counterparts, R4, R5, and R6, would result in the geometry seen in the *sple* eye disc and later in the adult eye. R1, R2, and R3 would be aligned vertically on the long (anterior) side of the eventual trapezoid, and R5 and R6 on the short (posterior) side, as in the normal eye, with the displacement of R4 providing the peak of the trapezoid. R1 and R6, used in our experiment to detect polarity in the disc, are late additions to the cluster, so their fates would likely be determined by the cells in the pre-existing five-cell precluster. Therefore, the anomalies in *sple* could arise earlier, e.g., by random switches in determination between R2 and R5 and their symmetrical counterparts R3 and R4.

DISCUSSION

Our results suggest that two different mechanisms establish the D/V distinction of the global eye field and the polarity of

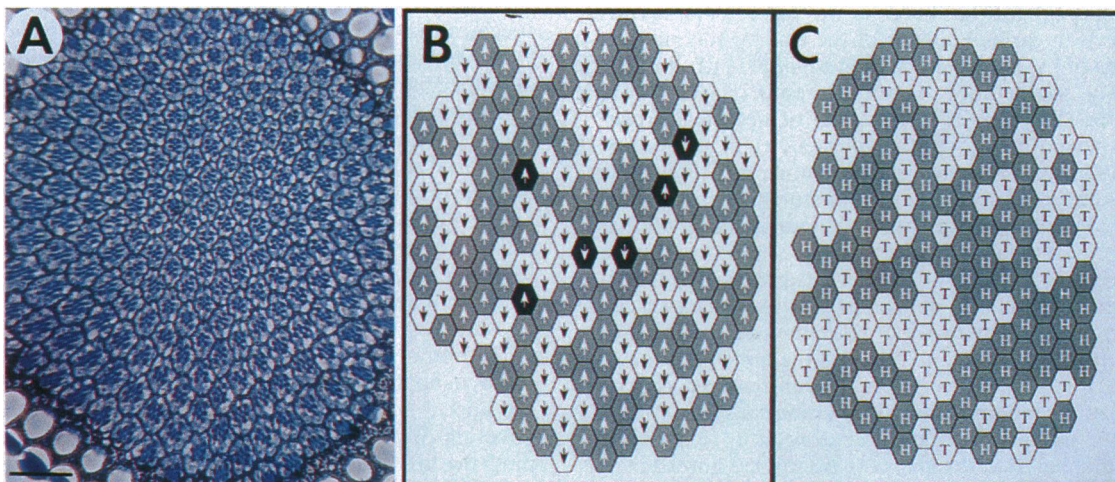


FIG. 2. Polarities in *sple* are essentially random. (A) Large area section of a *sple* eye (B). Dorsal (grey) and ventral (white) domains give the impression of local cooperativity. However, that is not real; such pseudodomains can occur by chance, as shown by the example in (C), where dorsal and ventral spins were assigned by tossing a coin. H, heads; T, tails. The solid ommatidia in B have A/P reversal. The anterior is to the right. (Bar = 30 μ m.)

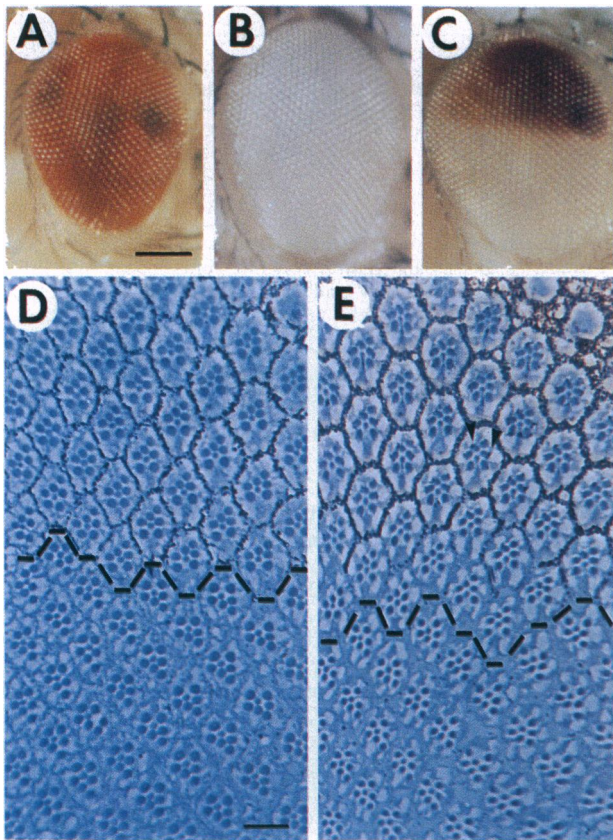


FIG. 3. Dorsal-specific *white*⁺ expression in an enhancer trap strain (*B1-12*) containing a *P-lacW* insertion. (A) Wild type. (B) *white* mutant. (C) Strain *B1-12* (heterozygous over balancer chromosome *TM3Sb*); expression of pigment is restricted to the dorsal domain. (D and E) Tangential sections of heterozygous *B1-12/TM3 Sb* and homozygous *B1-12/B1-12* eyes, respectively. Dotted lines denote the mirror image equator of symmetry. The boundary between *w*⁺ and *w*⁻ ommatidia coincides approximately with the equator, except that the *w*⁻ region sometimes extends dorsally by three ommatidial rows (E). No morphological abnormality was detected in the eyes of *B1-12* homozygous flies. The extension of the *w*⁻ region beyond the equator shown in Fig. 5E is not due to the homozygosity of the *B1-12* insertion; it is also found in heterozygotes. While the expression of *w*⁺ within photoreceptor cells in this strain is generally weak, when seen (pigment granules indicated by arrows), it is always dorsal-specific. (A–C, bar = 100 μ m; D and E, bar = 10 μ m.)

individual ommatidia. It has been shown that ectopic furrows can be induced in various regions of the disc by making *ptc*⁻ mosaic clones or by ectopic expression of *hh* (11, 12). In both cases, polarity and rotation of photoreceptor clusters were defined by the direction of progression of ectopic furrows, establishing new equators that are perpendicular to the furrows (5). This suggests that the ectopic retinal polarity can be established that is independent of a normal global D/V determinant. This is also consistent with our observation that the alteration of ommatidial polarity in *sple* does not affect a global D/V boundary marked with *w*⁺ expression. Interestingly, it was found that such dorsal-specific *w*⁺ expression can be altered by ectopic expression of *hh*: either derepression of *w*⁺ in the ventral portion or inhibition of the dorsal portion of the eye (5). However, a precise correlation between the *w*⁺ expression and the ommatidial orientation was not found, supporting the independent determination of *w*⁺ expression and ommatidial polarity. It remains to be studied how each of these is determined.

In each column of photoreceptor clusters behind the furrow, the process of clustering and differentiation starts at the center and proceeds distally to the polar regions of the disc. The

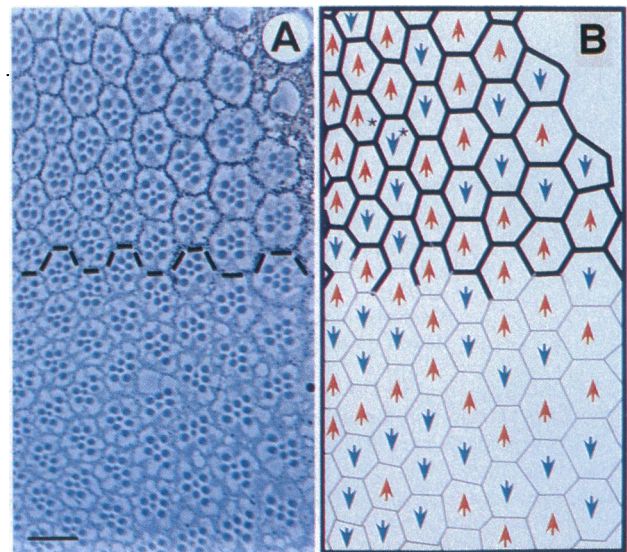


FIG. 4. Independence of expression of *sple* and *w*⁺. Eye of a *sple* fly containing the *B1-12* enhancer trap (*yw; sple; B1-12/TM3 Sb*). (A) Sectioned as in Fig. 1. (B) Schematic with arrows. Thick and thin grey lines represent *w*⁺ and *w*⁻ pigment cells, respectively. Dorsal and ventral orientations are indicated by red and green arrows, respectively. The polarities of many photoreceptor clusters are dorsoventrally reversed, as in *sple*, whereas the dorsal-specific *w*⁺ expression, as in *B1-12*, was unaffected by the *sple* mutation. Two ommatidia marked with asterisks had A/P reversals. The anterior is to the right. (Bar = 10 μ m.)

central position where the furrow and the equator meet [referred to as the “firing center” (11) or a “point source” of signal (5)] may send out a signal for ommatidial polarization. Such a signal may be provided by the *fz* gene that mediates center-outward signaling for ommatidial polarity (19).

In the normal eye, photoreceptor clusters rotate 90° in opposite directions above and below the equator, so that the long side of a trapezoid (R1–R2–R3) becomes anterior. In spite of D/V polarity reversals, most ommatidia in *sple* show correct anteroposterior polarity; the long side remains anterior. In contrast to *sple*, *fz* shows more complex phenotypes. For example, many ommatidia in the *fz* eye show A/P as well as D/V reversals and incomplete rotation of clusters (19), suggesting that the ommatidial polarity and the rotation may be directly or indirectly coupled by *fz*. In fact, *fz* regulates the expression of *nmo* (19), a gene that is required for normal rotation (3). *fz* may also regulate *sple*, which in turn controls specifically the D/V polarity of photoreceptor clusters.

As we proposed in Fig. 5, the D/V reversals in *sple* can be explained by cell fate switches between the equatorial (R1–R3) and the polar (R4–R6) cells and subsequent rotation. Normally, photoreceptor clusters rotate in a direction that leads equatorial cells (R1–R2–R3) to the anterior. For D/V but not A/P reversals to occur as in the *sple* eye, the D/V switches must be accompanied by reversed rotations: if the equatorial cells become R4–R5–R6 instead of R1–R2–R3, the cluster will rotate in the opposite direction to bring the R1–R2–R3 to the anterior. It appears that the direction of rotation is determined by the fates of the equatorial and the polar cells. Because dorsoventrally reversed photoreceptor clusters in the *sple* eye rotate in opposite directions, photoreceptor clusters in the *sple* eye appear to be able to respond normally to a cue for the direction of rotation. In contrast to *sple*, many ommatidia in the *fz* eye are reversed A/P as well as D/V. Such clusters in the *fz* eye may be abnormal in the specification of D/V cell fates as well as direction of rotation.

Mosaic analysis of *fz* indicated that the R3/4 pair is a critical determinant for the direction of rotation: *fz*⁺ cells become

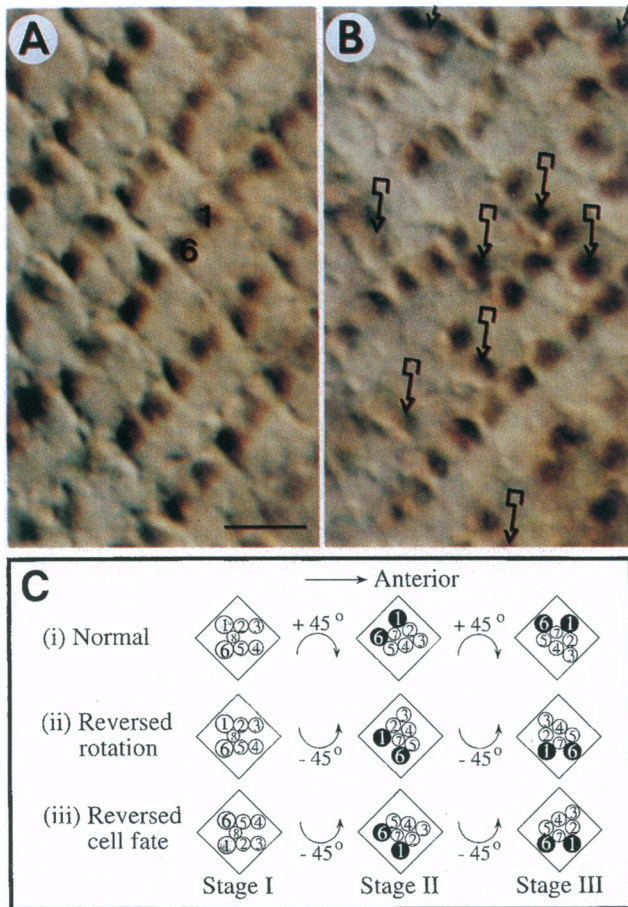


FIG. 5. Dorsoventral symmetry reversals in third instar larval developing *sple* eye disc. Anti-BarH1 antibody S12 was used to immunostain R1 and R6 cell nuclei. (A) Wild-type third instar eye disc; the clusters of photoreceptor precursors form a square-shaped array. In this ventral region view, R1 and R6 are regularly arranged at the posterior end of each photoreceptor cluster. (In the dorsal region, not seen here, they are in mirror symmetry to the ventral region.) (B) *sple* mutant eye disc. Dorsal and ventral cluster patterns coexist, so that BarH1 positive cells in many plain clusters are in mirror image to their normal positions. Squares with arrows indicate such positional changes. The anterior is to the right and the dorsal is to the top. (Bar = 10 μ m.) (C) A hypothesis for the dorsoventral reversal in *sple*. A developing cluster in the eye disc, below the equator, is taken as an example. Stage I, the early precluster, before rotation, consists of five cells (precursors of R3/4, R2/5, and R8) arranged in a symmetrical pattern, which is the same in both upper and lower halves of the disc. The future sites for R1 and R6, which have not yet joined the group, are indicated in gray. Stage II, after the cluster has rotated halfway. The now added R1 and R6 are shown in black, indicating staining by anti-Bar antibody. Stage III, after completion of the full 90° rotation. R8 is not shown in stages II and III, since R8 becomes basal to R7. (i) Normal eye disc. R1 is initially dorsal to R6, but as the cluster rotates to a total of 90° the long side of the trapezoid comes to face anteriorly. (ii) Reversed rotation hypothesis for aberrant ommatidium in the *sple* mutant. In that case, the long side of the trapezoid would become posterior to the short side, and the final trapezoid reversed both dorsoventrally and anteroposteriorly. However, almost all aberrant ommatidia in *sple* are reversed only dorsoventrally; the *sple* phenotype cannot be explained by reverse rotation. (iii) Reversed cell fate hypothesis. The initially dorsal cells in each cluster (R2 and R3) and their counterpart ventral cells (R5 and R4) assume fates that are reversed dorsoventrally. After addition of R1 and R6, followed by rotation (in normal direction), clusters in which this event has occurred will have polarity that is reversed dorsoventrally, but not anteroposteriorly.

anterior (19). This is consistent with an earlier notion that the breaking of symmetrical assembly of a photoreceptor cluster

into asymmetry occurs as R4 loses its contact with R8 resulting in the breaking of R3-R4 symmetry (26). It was also suggested that the *sple* function is required in R3, R4, or R5 for correct polarity of a photoreceptor cluster (19). These results suggest that an early distinction between R3 and R4 may be a key to establish the ommatidial polarity. The *fz* gene encodes a cell surface protein with seven transmembrane domains (27, 28). Because *sple* is likely to be a downstream component of *fz*, *sple* may be defective in translation of the polarity signal that is mediated by *fz*.

We thank Rosalind Young for excellent technical assistance. We also thank Kaoru Saigo and Tetsuya Kojima for anti-BarH1 antibody and the Indiana *Drosophila* Stock Center for *sple*¹. This work was supported by grants to S.B. from the National Science Foundation (MCB 9408718), the National Institutes of Health (EY 09278 and AG 12289), and the James G. Boswell Foundation.

1. Ready, D. F., Hanson, T. E. & Benzer, S. (1976) *Dev. Biol.* **53**, 217–240.
2. Wolff, T. & Ready, D. F. (1991) *Development (Cambridge, U.K.)* **113**, 841–850.
3. Choi, K.-W. & Benzer, S. (1994) *Cell* **78**, 125–136.
4. Bier, E., Vässin, H., Shepherd, S., Lee, K., McCall, K., Barbel, S., Ackerman, L., Carretto, R., Uemara, T., Grell, E., Jan, L. Y. & Jan, Y.-N. (1989) *Genes Dev.* **3**, 1273–1287.
5. Chanut, F. & Heberlein, U. (1995) *Development (Cambridge, U.K.)* **121**, 4085–4094.
6. Sun, Y. H., Tsai, C.-J., Green, M. M., Chao, J.-L., Yu, C.-T., Jaw, T. J., Yeh, J.-Y. & Bolshakov, V. N. (1995) *Genetics* **141**, 1075–1086.
7. Heberlein, U., Wolff, T. & Rubin, G. M. (1993) *Cell* **75**, 913–926.
8. Ma, C., Zhou, Y., Beachy, P. A. & Moses, K. (1993) *Cell* **75**, 927–938.
9. Pan, D. & Rubin, G. M. (1995) *Cell* **80**, 542–552.
10. Strutt, D. I., Wiersdorff, V. & Mlodzik, M. (1995) *Nature (London)* **373**, 705–709.
11. Ma, C. & Moses, K. (1995) *Development (Cambridge, U.K.)* **121**, 2279–2289.
12. Wehrli, M. & Tomlinson, A. (1995) *Development (Cambridge, U.K.)* **121**, 2451–2459.
13. Gubb, D., & Garcia-Bellido, A. (1982) *J. Embryol. Exp. Morphol.* **68**, 37–57.
14. Heitzler, P., Coulson, D., Saenz-Robles, M. T., Ashburner, M., Roote, J., Simpson, P. & Gubb, D. (1993) *Genetics* **135**, 105–115.
15. Gubb, D. (1993) *Development (Cambridge, U.K.)* Suppl., 269–277.
16. Theisen, H., Purcell, J., Bennett, M., Kansagara, D., Zuhuriidin, A. & Marsh, J. L. (1994) *Development (Cambridge, U.K.)* **120**, 347–360.
17. Vinson, C. R. & Adler, P. N. (1987) *Nature (London)* **329**, 549–551.
18. Adler, P. N. (1992) *BioEssays* **14**, 735–741.
19. Zheng, L., Zhang, J. & Carthew, R. W. (1995) *Development (Cambridge, U.K.)* **121**, 3045–3055.
20. Lindsley, D. L. & Zimm, G. G. (1992) *The Genome of Drosophila melanogaster*. (Academic Press, San Diego).
21. McLean, I. W. & Nakane, P. K. (1974) *J. Histochem. Cytochem.* **22**, 1077–1108.
22. Higashijima, S.-I., Kojima, T., Michiue, T., Ishimaru, S., Emori, Y. & Saigo, K. (1992) *Genes Dev.* **6**, 50–60.
23. Choi, K.-W. & Benzer, S. (1994) *Neuron* **12**, 423–431.
24. Franceschini, N. & Kirschfeld, K. (1971) *Kybernetik* **8**, 1–13.
25. Tomlinson, A. & Ready, D. F. (1987) *Dev. Biol.* **120**, 366–376.
26. Tomlinson, A. (1985) *J. Embryol. Exp. Morphol.* **89**, 313–331.
27. Vinson, C. R., Conover, S. & Adler, P. N. (1989) *Nature (London)* **338**, 263–264.
28. Park, W. J., Liu, J. & Adler, P. N. (1994) *Mech. Dev.* **45**, 127–137.